Promising new wavelengths for multi-photon fluorescence microscopy: thinking outside the Ti:Sapphire box

Greg Norris[1], Rumelo Amor[1], John Dempster[1], William B. Amos[2] and Gail McConnell[1*]

[1] Centre for Biophotonics, SIPBS, University of Strathclyde, 161 Cathedral Street, Glasgow G4 0RE, UK.
[2] Medical Research Council Laboratory of Molecular Biology, Hills Road, Cambridge CB2 0QH, UK.
* Corresponding author email: g.mcconnell@strath.ac.uk
Telephone: 00 44 141 548 4805
Fax: 00 44 141 548 4887.

Keywords: Multi-photon, live cell, cytoplasmic streaming.

ABSTRACT

Multi-photon excitation (MPE) imaging is dominated by the Ti:Sapphire laser as the source for excitation. However, it is limited when considering 3PE of common fluorophores and efficient 2PE of UV dyes which require wavelengths beyond the range of the Ti:Sapphire. Two ultra-short pulsed sources are presented as alternatives: a novel optical parametric oscillator (OPO) geometry (1400–1600nm) and the sum-frequency mixing of an OPO and Yb-doped fibre laser, providing a tunable output (626-635nm).

For long wavelengths, we report three-photon laser scanning microscopy (3PLSM) using a bi-directional pumped optical parametric oscillator (OPO) with signal wavelength output at 1500 nm. This novel laser was used to overcome the high optical loss in the infrared spectral region observed in laser scanning microscopes and objective lenses that renders them otherwise difficult to use for imaging. To test our system, we performed 3PLSM auto-fluorescence imaging of live plant cells at 1500 nm, specifically Spirogyra, and compared performance with two-photon excitation (2PLSM) imaging using a femtosecond pulsed Ti:Sapphire laser at 780 nm. Analysis of cell viability based on cytoplasmic organelle streaming and structural changes of cells revealed that at similar peak powers, 2PLSM caused gross cell damage after 5 minutes but 3PLSM showed little or no interference with cell function after 15 minutes. The 1500 nm OPO was thus shown to be a practical laser source for live cell imaging.

For short wavelengths, we report the use of an all-solid-state ultra-short pulsed source specifically for two-photon microscopy at wavelengths shorter than those of the conventional Ti:Sapphire laser. Our approach involved sum-frequency mixing of the output from the long-wavelength OPO described above with residual pump radiation to generate fs-pulsed output in the red spectral region. We demonstrated the performance of our ultra-short pulsed system using fluorescently labelled and autofluorescent tissue, and compared with conventional Ti:Sapphire excitation. We observed a more than 3-fold increase in fluorescence signal intensity using our visible laser source in comparison with the Ti:Sapphire laser for two-photon excitation at equal illumination powers of 22 mW or less.

Multiphoton Microscopy in the Biomedical Sciences XIII, edited by Ammasi Periasamy, Karsten König, Peter T. C. So,
Proc. of SPIE Vol. 8588, 858802 · © 2013 SPIE · CCC code: 1605-7422/13/$18 · doi: 10.1117/12.2008189

INTRODUCTION

Scanning microscopy using two-photon excitation of fluorescence is well established. However, it is desirable to explore the potential of three-photon processes, which are relatively little studied. It may be that researchers have been deterred by the requirement for higher peak intensities predicted from theory for three-photon excitation[1], and fear of heating of the specimen because of higher absorption in aqueous media[2]. However, a possible advantage of using three photons rather than two is that longer wavelengths can be used, possibly with less cytotoxic effect, and the resolution loss that results from the longer wavelength can be to some extent reversed by the intensity-cubed dependence of the three-photon excitation process[3].

Some promising results have already been obtained for three-photon laser scanning microscopy (3PLSM) using third harmonic generation[4-8]. For example, by increasing the wavelength to λ=1260 nm with a femtosecond-pulsed Cr:Forsterite laser, an improved depth of tissue imaging by third harmonic generation has been achieved[9,10] and three-photon excitation laser scanning fluorescence has been demonstrated[11] for a range of samples, albeit at shorter (λ<1100 nm) wavelengths. It is significant that the peak intensities used for 3PLSM in these reports were similar to those routinely used in two-photon laser scanning microscopy (2PLSM), and excessive damage to the specimen was not seen.

For three-photon excitation of fluorophores with single-photon absorption in the visible region of the spectrum, wavelengths are needed which are above the range of the ubiquitous Ti:Sapphire laser[12] and the Cr:Forsterite laser, so, in this work, we have examined excitation at λ=1500 nm. Unfortunately, few suitable lasers exist with such long-wavelength emissions. A fibre laser has been used[7] to record third-harmonic images from plant leaves, but fluorescence emission was not studied. The fibre laser is also fixed wavelength, which is a drawback for fluorescence excitation. Wavelength tuning in the required spectral region is most frequently achieved using expensive commercial optical parametric oscillators (OPOs) synchronously pumped by a similarly high-cost femtosecond-pulsed Ti:Sapphire laser. However, the frequency conversion process is often inefficient and the average power from these systems at λ=1500 nm is often too low to overcome the poor transmission of microscope objectives at infrared wavelengths[13]. Increasing the output power of an OPO, even with careful thermal management, is not straightforward. Nonlinear crystals typically have much lower damage thresholds than laser gain material[14] and this limits the peak intensity that can be used to pump a femtosecond-pulsed OPO. Therefore, in spite of the very high peak intensities available from pump lasers, only a fraction may be applied in single-pass pumped OPO systems.

There exist many synthetic and naturally occurring fluorescent molecules with sub-λ=360 nm single-photon excitation peaks, including Indo-1, DAPI (4',6-diamidino-2-phenylindole) Hoechst Blue, NADH, tryptophan and phenylalanine[15-17]. Single photon excitation could be applied for these molecules, with current diode technology allowing this to be done at low cost[18]. However, intrinsic issues with working in the UV range, i.e. sample damage and the requirement for specialized UV optics, make this approach unattractive. Two-photon excitation offers a route to by-pass this harmful spectral range and can be applied to many commercial microscopes. However, due to the of a lack of inexpensive ultra-short pulsed laser sources at wavelengths shorter than those of the Ti:Sapphire, little is known of the two-photon excitation dynamics at wavelengths between λ=600 and 650 nm. Such two-photon Ti-sapphire excitation spectra that are available show the two-photon excitation cross-section increasing towards shorter excitation wavelengths[1, 19, 20].

We report the development of a novel bi-directional synchronously pumped femtosecond-pulsed OPO system for both 3PLSM and short-wavelength 2PLSM. This system provides a much higher peak output power than the conventional single-pass pumped OPO geometry, and hence is ideally suited to compensate for the high optical power loss of laser scanning microscopes at long wavelengths. Furthermore, by using an inexpensive fibre laser as the pump source, the total cost of our system, including laser, OPO and microscope, is less than that for a femtosecond-pulsed Ti:Sapphire laser alone. We have applied the system to 3PLSM and 2PLSM at long and short wavelengths respectively. Firstly, we performed long wavelength imaging of auto-fluorescence in live plant cells, specifically those of the alga *Spirogyra*, and compare performance with 2PLSM imaging using a standard, commercially available femtosecond-pulsed Ti:Sapphire laser. Secondly, we used the short-wavelength source laser for 2PLSM of fluorescently labelled tissue and naturally occurring fluorophores, and again perform a comparison with conventional Ti:Sapphire excitation.

EXPERIMENT

The laser system

A schematic diagram of the OPO system at the heart of our imaging experiments is shown in Figure 1.

Full details on the theory and operation of the bi-directional pumped OPO system are available[21], and hence we present only a brief overview of the experimental geometry here.

We used a continuous wave mode-locked Yb-doped fibre laser, with an average power of 2W and repetition rate of 80 MHz, pulses of 260 fs duration at a wavelength of λ=1064 nm and with a spectral width of 12 nm (FWHM) (Femtopower 1060-2-s, Fianium, Southampton, UK). By blocking the pump beam between elements 3 and 12, we refer to the direction of pumping as the 'forward' direction, or by blocking the pump between elements 3 and 4, it is referred to as the 'reverse' direction. This is as per a traditional single-pass pumping scheme. With all beam paths open and unblocked, bi-directional pumping, i.e. using both the forward and reverse pass pump beams, was possible.

In order to keep the peak intensity of the pump source below the damage threshold intensity of the nonlinear crystal, only 50% of the average power from the pump was used in a single-pass in both the forward and reverse directions. By using a 50/50 thin-plate beam-splitter (element 3), 1 W of average power was therefore provided in both the forward and reverse pumping directions.

The polarizations of both pump beams were independently controlled by half-wave plates (elements 4, 17) designed for use at the pump wavelength of λ=1064 nm. Both pump beams were then mode-matched to the linear OPO cavity using two sets of anti-reflection coated spherical lenses (elements 5, 6, 18, 19). The lenses were used to provide a pump beam radius of 20 um in both the forward and reverse direction, which was determined by consideration of the Boyd-Kleinman focusing parameter[14].

Elements 15 and 16 were highly-reflective dielectric mirrors at the pump wavelength, which were mounted on a single translation stage. This created a time delay, permitting temporal displacement of the pump pulse in the reverse direction relative to the circulating signal wavelength pulse. This was used to ensure synchronicity of the system in both forward and reverse directions. Additionally, mirror 10 was placed on a translation stage to control synchronization of resonating signal wavelength pulses.

A 3 mm long periodically poled lithium niobate (PPLN) crystal (element 8) was designed to provide maximum output power at an OPO signal wavelength of λ=1500 nm. Wavelength tuning of the OPO was possible from λ=1400 nm to λ=1650 nm by using the range of periods available in the PPLN crystal and also by adjusting the temperature of the PPLN, but a fixed wavelength of λ=1500 nm was used for our experiments as this gave the highest intensity fluorescence signal from the *Spirogyra* specimen. All of the mirrors in the OPO resonator were designed to be highly reflective at the signal wavelength and highly transmitting at pump and idler wavelengths, with the exception of the output coupler (element 11), which had a reflectivity of 50% at the signal wavelength. Elements 7 and 9 were zero lens mirrors with a radius of curvature of 100 mm, with the cavity designed to provide a spot size of 19 um inside the PPLN crystal. Zero lens mirrors have the same radius of curvature on both surfaces, so a beam propagating through the element is not focused or defocused, making it easier to design the optical system and control the beam.

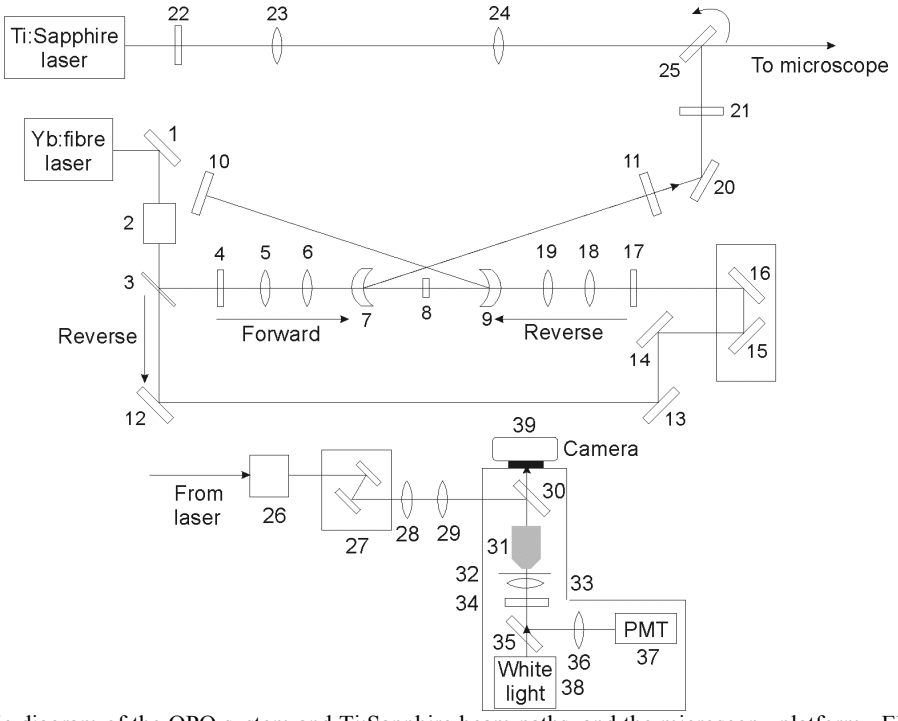

Figure 1. A schematic diagram of the OPO system and Ti:Sapphire beam paths, and the microscopy platform. Elements 1 and 12-16 are highly reflecting plane mirrors at the pump wavelength of λ =1064 nm. 2 is a Faraday isolator. 3 is a 50/50 thin-plate beamsplitter at λ=1064 nm. 4 and 7 are half-wave plates at λ=1064 nm. 5, 6, 18 and 19 are mode-matching lenses. 7 and 9 are zero lens ROC=100mm mirrors (zero lens mirrors have the same radius of curvature on both surfaces, so a beam propagating through the element is not focused or defocused, making it easier to design the optical system and control the beam), highly transmitting at λ=1064 nm and highly reflecting at λ=1500 nm. 8 is a 3mm long PPLN crystal. 10 and 20 are high reflectivity plane mirrors at λ=1500 nm, and 11 is a 50% reflectivity mirror at λ=1500 nm, which serves as the OPO output coupler. 21 is a λ=1400 nm long pass filter. 22 is an attenuator for use at λ=780 nm, and 23 and 24 are lenses to shape the output of the Ti:Sapphire laser to match the profile of the OPO beam. 25 is a high-reflectivity plane mirror at λ=1500 nm, placed in a flip mount to enable easy switching between the λ=780 nm and λ=1500 nm beams. Item 26 is a periscope comprising two broadband infrared reflecting mirrors, and 27 is the scanning system, comprising two galvo mirrors. Item 28 is the f=80mm scan lens and item 29 is the f=160mm tube lens. 30 is a beam-steering mirror and 31 is the 40x/1.3 N.A. objective lens. 32 is the specimen and/or specimen plane. 33 is the condenser lens and 34 is a filter holder containing the λ=700 nm short-pass and λ=629 ± 26.5 nm bandpass filter. 35 is a switch-in reflector, used to send the transmitted fluorescence signal to a collecting lens (36) and then the photomultiplier tube, element 37. 38 is a white-light source, used to illuminate the specimen for bright-field images, captured by 39, a 5 megapixel CMOS camera.

The PPLN damage threshold intensity was experimentally demonstrated to be 4 GW/cm^2, which, when considering the pump source described previously, corresponded to a maximum single-pass pump average power of 1.1 W and a peak power of 49 kW. The PPLN crystal was anti-reflection coated at the pump wavelength on one surface only, namely the surface closest to element 9, due to the crystal being a section cut from a longer PPLN crystal for this study. Neither crystal surface was anti-reflection coated at the signal or idler wavelengths. This resulted in a substantial optical loss and which was therefore detrimental to the overall conversion efficiency. The crystal was kept in a home-made oven at a temperature of 140 ^{o}C to ensure fixed signal wavelength operation.

The output of the OPO (either single-pass or bi-directional) was then coupled into a home-built laser scanning microscope platform. This is shown in the lower half of Figure 1. Element 21 was a band-pass filter (FB1500-12, Thorlabs, Ely, UK), used to ensure that residual pump wavelength radiation at λ=1064 nm was blocked and only the signal wavelength output at λ=1500nm served as the excitation source for 3PLSM.

Two mirrors and a periscope system were used to steer the signal wavelength radiation towards the scanning system. The scan head module was mounted on an elevated breadboard at the back of the microscope.

The scan head comprised of two galvanometer-driven mirrors mounted at right angles to one another. The 5-mm XY mirror set, XY mount bracket, galvanometer scanners, MicroMax 671XX series driver circuit boards to control the galvanometers and interconnect cables were obtained from Cambridge Technology, Lexington, Massachusetts, USA. This system was capable of speeds of up to 1 kHz and scan angles of up to ± 20 degrees. The mirrors used a protected silver coating on a fused silica substrate with a flatness of λ/4. The XY mount bracket was placed on an XY translation stage for optimum positioning of the mirrors relative to the excitation beam. The power supply units for the driver circuit boards were obtained from XP Power GmbH, Bremen, Germany.

The output beam from the scanning was focused through an achromatic doublet with a focal length of f=+80 mm (80 DQ 25, Comar, Cambridge, UK) serving as the scan lens. The scan lens was positioned 80 mm from the midway point between the scanning mirrors on one side and 80 mm from the intermediate image plane of the tube lens on the other side. The tube lens was an achromatic doublet with a focal length of f=+160 mm (160 DQ 25, Comar, Cambridge, UK). This element was placed 160 mm from the intermediate image plane and therefore 240 mm from the scan lens on one side and 160 mm from the back aperture of the objective lens. The scan lens and tube lens combination doubled the beam width so that the back aperture of the objective lens was consistently overfilled. We used a 40x/1.3 NA objective lens (S Fluor, Nikon, UK) in the excitation path, and a NA=0.9 condenser lens in the transmission path. In these experiments we used a single λ=700 nm short-pass filter (et700sp-2p8, Bellows Falls, Vermont, USA) and λ=629 ± 26.5nm bandpass filter (FF01-629/53-25, Laser 2000, Ringstead, UK) in the transmission path to block the excitation wavelength and any harmonic generation, such that only auto-fluorescence from the specimens was transmitted. A photomultiplier tube (RFI-QL-30F, Thorn EMI, London, UK) was employed to collect the fluorescence signal. To control the scanning galvo mirrors and for image capture, we used the freely available MPScope software developed by[22]. For all experiments, the image size was 512 x 512 pixels taken at 2.18 frames per second, with a pixel dwell time of 1.4 μs.

Figure 2 shows the system modified for short-wavelength performance. The same continuous wave mode-locked Yb-doped fibre laser served as the pump source, with an average power of 2 W and repetition rate of 80 MHz, pulses of 260 fs duration at a wavelength of λ=1064 nm and with a spectral width of 12 nm (FWHM) (Fianium, Femtopower 1060-2-s). This laser was split into two components by a 50/50 beamsplitter (element 3). The first beam was used to synchronously pump an optical parametric oscillator (OPO), the output of which was recombined spatially and temporally with the second pump beam in a second nonlinear optical crystal to perform sum-frequency mixing (SFM).

The output from the OPO was then propagated through a variable neutral density filter (element 12) and a long-pass filter (Thorlabs FB1400-12 (element 13)) to ensure that residual pump wavelength radiation at λ=1064 nm was blocked and only the signal wavelength output at λ>1400 nm was available for the SFM process. Element 14 was a highly reflecting mirror at the signal wavelength and elements 15 and 16 were a half-wave plate to control the polarisation of the OPO and a f=+80 mm convex lens to facilitate beam-shaping of the signal wavelength output prior to the SFM process.

The benefit of using an OPO as one of the pump sources for SFM was the ability to vary the wavelength and to optimise the phase-matching conditions. In conjunction with the control of the temperature of the SFM PPLN crystal, the wavelength of the output could be altered whilst maintaining a zero phase mis-match.

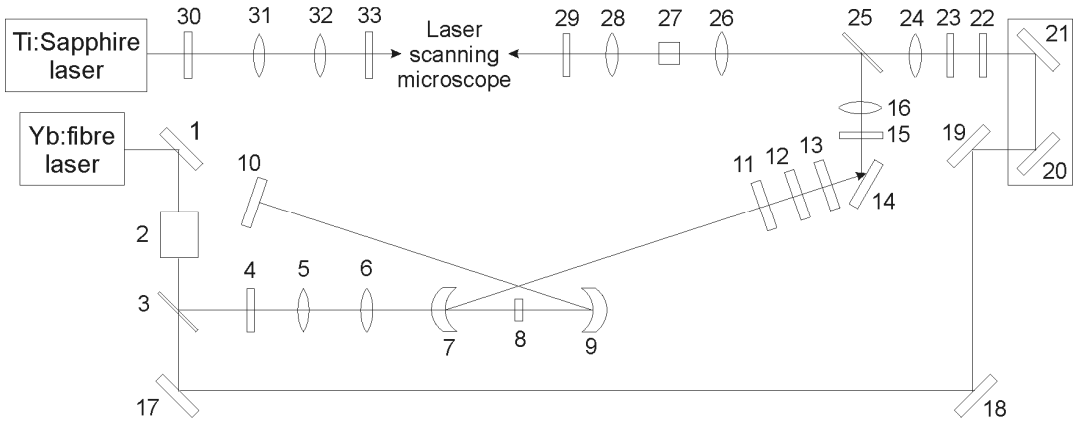

Figure 2. A schematic diagram of the OPO system and Ti:Sapphire beam paths used to generate ultra-short pulsed red light via SFM. Elements 1 and 17-21 are highly reflecting plane mirrors at the pump wavelength of λ=1064 nm. 2 is a Faraday isolator. 3 is a 50/50 thin-plate beamsplitter at λ=1064 nm. 4 is a half-wave plates at λ=1064 nm. 5 & 6 are mode-matching lenses. 7 and 9 are zero lens ROC=100 mm mirrors (zero lens mirrors have the same radius of curvature on both surfaces, so a beam propagating through the element is not focused or defocused, making it easier to design the optical system and control the beam), highly transmitting at λ=1064 nm and highly reflecting at λ=1500 nm. 8 is a 3 mm long PPLN crystal. 11 is a 50% reflectivity mirror at λ=1500 nm, which serves as the OPO output coupler. 12 is a half-wave plate at λ=1500 nm and 13 is a variable neutral density filter. 14 is a high reflectivity plane mirror at λ=1500 nm, and 15 is a long-wave pass filter. 22 is a variable neutral density filter for use at λ=1064 nm, 23 is a half-wave plate at λ=1064 nm and 24 is a lens. 25 is a high-reflectivity plane mirror at λ=1500 nm that is highly transmitting at λ=1064 nm. 26 is a lens, 27 is the PPLN crystal for SFM of λ=1064 nm and the OPO. 28 is a collimating lens and 29 is a half-wave plate for use with visible wavelengths. Element 30 is a half-wave plate for use with the Ti:Sapphire wavelengths. 31 and 32 are lenses to shape the beam and 33 is a neutral density filter for use with the Ti:Sapphire laser.

We now consider the second pump beam used for the SFM process, Elements 17, 18 and 19 were used to steer the beam towards a trombone arrangement. This comprised two highly-reflective dielectric mirrors at the pump wavelength, which were mounted on a single linear translation stage (elements 20 and 21). This created a time delay, permitting temporal displacement of the pump pulse, which was used to synchronise the pump pulse and signal wavelength pulse from the OPO within the nonlinear material for SFM. Elements 21 and 22 were variable neutral density filter to control the intensity of the radiation reaching the SFM arrangement and a f=+100 mm lens to shape the signal wavelength output prior to the SFM process.

The pump and signal wavelength beams were combined at element 23, which was a plane mirror highly reflecting at the signal wavelength and highly transmitting at the pump wavelength, similar to element 10, used as a cavity end mirror in the OPO. The two beams were then spatially and temporally overlapped and focused using a single f=+25 mm spherical lens, anti-reflection coated for at λ=1000-1600 nm for minimal power loss (element 24). This focused both beams into a 1 mm long PPLN crystal, this time with a domain period length of 11.12 to 11.22 μm, designed for SFM of the pump and signal wavelengths. The sum-frequency mixed output was then collimated using a f=+25 mm spherical lens, this time anti-reflection coated at λ=400-800 nm (element 26). Element 27 was a λ=700 nm short-wave pass filter (ET700sp-2p8, Chroma Technology, USA) to block the pump and signal wavelength outputs, and transmit the sum-frequency mixed wavelength only. This was then directed towards the same home-built laser scanning microscope as described previously.

For comparison with existing technology, the output from a commercial ultra-short pulsed Ti:Sapphire laser was also coupled into the laser scanning microscope. The polarisation of the Ti:Sapphire laser was fine-tuned using a half-wave plate designed for operation at wavelengths λ=700-1050 nm (element 30), and the beam shaped using spherical lenses of f=+100 mm and f=+150 mm (elements 31 and 32) to match the beam profile of the sum-frequency mixed source. The average power of the Ti:Sapphire laser exceeded 200 mW across the tuning range, and so a variable neutral density filter (element 33) was used to ensure the delivery of the same peak intensity to the specimen as was provided by the sum-frequency mixed source. All optical properties of the OPO, sum-frequency mixed and Ti:Sapphire lasers were identical where possible, including, importantly the peak power at the specimen plane. The Ti:Sapphire was operated at a

wavelength of λ=720 nm and gave a pulse duration of 250 fs at a repetition rate of 76 MHz. The Ti:Sapphire beam was expanded to provide a similar beam diameter to the TEM00 sum-frequency mixed output to fill the back aperture of the objective lens.

Live specimens: long wavelength imaging

To test our long wavelength system with a living cellular specimen, we imaged preparations of *Spirogyra*, a eukaryotic green alga with cylindrical cells joined end-to-end to form a filament. The advantage of this material is that every cell and even individual cytoplasmic organelles within it can be imaged clearly. The cylindrical cell shape is maintained by a cell wall containing pectin and cellulose. In *Spirogyra*, the cytoplasm exists as a thin layer between the cell wall and a central vacuole, and ribbon-like chloroplasts are present within the cytoplasm and arranged in a characteristic helical form. The single-photon excitation and emission auto-fluorescence properties of chlorophyll are well-known and understood, with an excitation maximum of around λ=450 nm and peak emission wavelength of λ=680 nm, depending on whether the chlorophyll is type a or b[23, 24]. *Spirogyra* filaments were mounted in water and placed between a slide and a coverslip for imaging, using silicone grease as a gas-permeable sealant to retard evaporation and fix the coverslip to the slide. With this specimen, we performed 3PLSM using both the single-pass and bi-directional pumped OPO geometries to excite auto-fluorescence, and bright-field transmission imaging to monitor cellular viability.

As a measure of cell viability, we recorded active movement of organelles via cytoplasmic streaming[25, 26] at 5 minute intervals using conventional brightfield imaging and a CMOS camera (GXCam-5, GX Optical, Haverhill, UK), and recorded any structural changes to the cell following irradiation for 2PLSM and 3PLSM. The 5 minute duration was chosen only to represent the duration of a routine imaging experiment. Cytoplasmic streaming is unique to plant cells while mammalian cells use microtubules to transport vesicles. In living plant cells, cytoplasmic organelles are visible in active movement, easily distinguished from Brownian motion by its directional nature, with groups of organelles frequently visible progressing in tandem along defined tracks. The organelles appeared spherical or capsule-shaped and probably included proplastids and mitochondria, which could be seen in clearer contrast if the condenser aperture of the microscope was closed down substantially. It is known that in such cells, streaming occurs at the expense of endogenous cellular energy reserves, and is a good measure of cell health[25].

Live specimen: short wavelength imaging

To test our system, we imaged a live preparation of *Hosta* sp leaf lower epidermis, with a thickness of less than 100 μm. The plant leaf was chosen to test whether the short wavelength of the new laser would show a characteristic fluorescence pattern in spite of the complexity of the living material. We chose this specimen to test whether short-wavelength two-photon excitation has any useful specificity, in view of the possibility that tyrosine and tryptophan fluorescence might make almost all proteins fluoresce at these novel wavelengths, as happens with single photon short-wavelength ultraviolet excitation. We note that this sample was relatively thin: if thicker tissues were to be imaged, it would be advisable to couple our system with a method of pre-dispersion compensation to compensate for any pulse broadening incurred within a sample, such as that provided by current commercial systems.

RESULTS

Long wavelength imaging

Figure 3(a) shows 3PLSM images of *Spirogyra* using the bi-directional pumped OPO. With the maximum average power from the single-pass geometry, no useful fluorescence signal was detected. However, with a minimum average power of 27 mW from the bi-directional pumped OPO, three-photon excitation of auto-fluorescence was possible. Figure 3(b) shows a three-dimensional auto-fluorescence reconstruction of the *Spirogyra* chloroplast, obtained using an average power of 31 mW at the specimen. The plot in Figure 3(c) confirms the three-photon nature of the auto-fluorescence excitation process, with a gradient of 3.3 measured from n=5 regions at n=12 power levels. Since it is known that plant cells can scatter a third harmonic when irradiated at these wavelengths (Millard *et al*, 1999) a barrier filter at the appropriate lower bandpass (500 ± 25 nm) was tested and it was established that the chloroplast-specific

emissions in the red spectral region were auto-fluorescence, not third harmonic. We note that the auto-fluorescence emission intensities for both two-photon and three-photon imaging were comparable for similar input powers used.

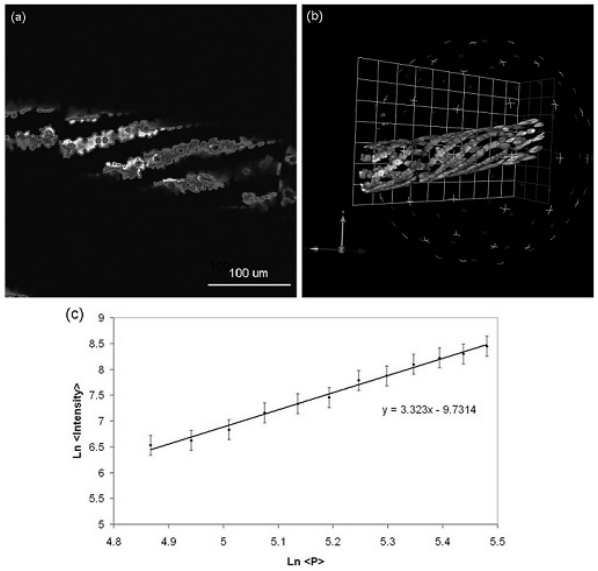

Figure 3. (a) A cross-sectional auto-fluorescence image of *Spirogyra* taken using the bi-directional pumped OPO at λ=1500 nm, and with an average power of 31mW at the specimen. The bright bands with serrated edges are optical cross sections of the chloroplasts. The dark circular spots visible at intervals along the chloroplasts are pyrenoids (carbohydrate reserve granules characteristic of this genus of alga). (b) Three-dimensional auto-fluorescence reconstruction of *Spirogyra* (Volocity, Improvision). The unit cell of the grid is 28.03 μm. (c) Log-log plot with a gradient of 3.3 confirms the three-photon nature of the auto-fluorescence excitation.

Figure 4 presents data from a comparison of the Ti:Sapphire at a wavelength of λ=780 nm for 2PLSM and the bi-directional pumped OPO at a wavelength of λ=1500 nm for 3PLSM. The bright-field images are shown from time t=0 mins in 5 minute increments to 15 mins for continuous irradiation with (a) the Ti:Sapphire and (b) the OPO system. At time t=0 mins, i.e. prior to irradiation, both specimens appeared healthy and cytoplasmic organelle streaming was evident in brightfield. This was confirmed by capturing movies at 8 frames per second, using the brightfield transmission image. The initial velocity of the organelles at t=0 was measured to be 12.7 μm ± 1.8 μm for the sample subsequently irradiated with the Ti:Sapphire laser, and 13.6 μm ± 2.7 μm for the sample later irradiated with the bi-directional pumped OPO. At time t=5 mins of constant irradiation, the sample imaged using the Ti:Sapphire for 2PLSM showed significant structural damage to the chloroplasts within the cytoplasm, and no cytoplasmic organelle streaming was visible. By comparison, even after t=15 mins of constant irradiation, the sample imaged using 3PLSM using the OPO at λ=1500 nm remained structurally unchanged and cytoplasmic organelle streaming continued unabated.

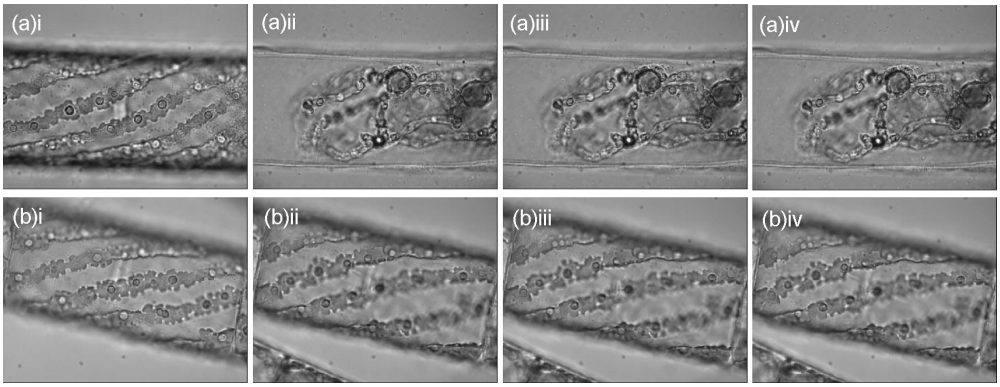

Figure 4(a) Brightfield images of *Spirogyra* taken after constant irradiation with the femtosecond-pulsed λ=780 nm Ti:Sapphire laser for time periods of (i) t=0 mins, (ii) t=5 mins, (iii) t=10 mins and (iv) t=15 mins. 3(b) shows brightfield images for the same

irradiation times using the femtosecond-pulsed bi-directionally pumped OPO at λ=1500 nm. The difference in colour is merely due to a different white balance setting of the camera.

Short wavelength imaging

Our apparatus gave a sum-frequency mixed wavelength tunable from λ=620-636 nm. Figure 5 shows the average output power corresponding to input OPO wavelength while varying the temperature of the SFM PPLN crystal.

The maximum average output power from the SFM process was 150 mW at a wavelength of λ=630 nm with a beam quality of $M^2 \sim 1.3$. This condition corresponded to mixing of the λ=1064 nm output from the pump laser with λ=1538 nm radiation from the OPO, and a SFM PPLN crystal temperature of 418 K with a period length of λ=11.7 μm. Tuning of the OPO signal wavelength was achieved by a combination of temperature tuning and OPO PPLN period length selection. Signal wavelengths below λ=1500 nm and above λ=1570 nm generated negligible powers. This was also the case for SFM PPLN crystal temperatures below 398 K and above 428 K.

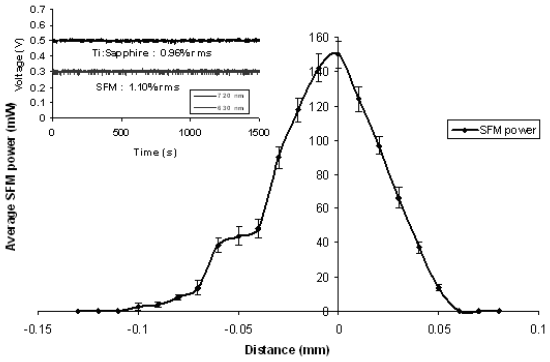

Figure 5. Average power at a sum-frequency mixed wavelength of λ=630 nm (1064 nm + 1550 nm) as a function of temporal overlap of the two input wavelengths within the SFM PPLN crystal. *Inset:* Comparison of the stability of the SFM source, measured at the peak output power, and the commercial Ti:Sapphire laser.

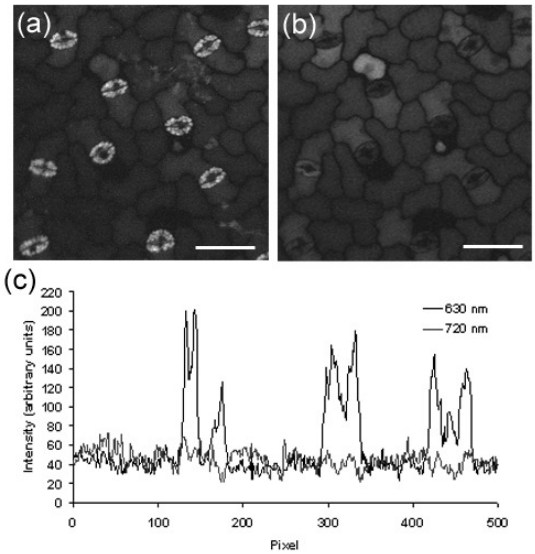

Fig 6. (a) Fluorescence image of live *Hosta* sp leaf epidermis using the sum-frequency mixed λ=630 nm source for two-photon excitation. (b) Fluorescence image of the same region of live Hosta sp using a Ti:Sapphire laser source at a wavelength of λ=720 nm source for two-photon excitation. In (a) the stomata are clearly visible because of guard cell autofluorescence, whereas in (b) there is higher background but less specificity. (c) A typical example of an intensity line scan passing through three guard cells was extracted using ImageJ. It was found that regions containing guard cells in n=10 images, more than a 3-fold increase in fluorescence signal

intensity was observed when using the red light at λ=630 nm in comparison with the λ=720 nm Ti:Sapphire laser for two-photon excitation. Scale bars correspond to 50 microns.

Figure 6 shows two-photon excitation images of the *Hosta* sp leaf epidermis showing autofluorescence. Figure 6(a) was captured using the sum-frequency mixed source at λ=630 nm and Figure 6(b) was obtained using the Ti:Sapphire laser source at λ=720 nm. The peak power used to acquire the images was 0.95 kW, with the same peak power provided at the specimen plane from the two sources. Using ImageJ to analyse the fluorescence signal intensity from comparable line scans containing the guard cells in n=10 images, we observed more than a 3-fold increase in fluorescence signal intensity using the red light at λ=630 nm in comparison with the λ=720 nm Ti:Sapphire laser for two-photon excitation. With the Ti:Sapphire laser source, there was a slightly higher level of background auto-fluorescence but the stomata are not clearly visible. However, the shorter-wavelength sum-frequency mixed source gave a much improved signal to background ratio for studying the stomata present within the specimen. The autofluorescence seems likely to be due to chlorophyll. In view of the finding that chlorophylls emit in the blue after 2-photon excitation at λ=650-680 nm[27] it would be of interest to study the fluorescence of chlorophyll at the shorter wavelengths supplied by our laser.

CONCLUSION

In summary, we have reported the use of an optical parametric oscillator based system for long and short wavelength multi-photon microscopy.

Using the higher average and peak powers from this bi-directional OPO, we overcame the >70% optical loss in the infra-red spectral region observed in the laser scanning microscope and objective lenses that renders these systems otherwise difficult or impossible to use for long wavelength excitation imaging. Furthermore, by using an inexpensive fibre laser as the pump source rather than a Ti:Sapphire, the total cost of our system, including laser, OPO and microscope, is almost an order of magnitude less than a commercial Ti:Sapphire, OPO and laser scanning microscope package.

We performed 3PLSM of live *Spirogyra* cells using the bi-directional pumped OPO and compared auto-fluorescence imaging capability with 2PLSM using a standard commercial femtosecond pulsed Ti:Sapphire laser at a wavelength of λ=780 nm, with care taken to match the peak and average powers from both lasers. With the λ=780 nm Ti:Sapphire laser, gross structural damage was observed after t=5 mins of continuous irradiation, while the λ=1500nm bi-directional OPO gave a notable improvement in cell viability: it had no effect on the structure of the chloroplasts, and cytoplasmic organelle streaming velocities were preserved over t=15 mins of constant irradiation.

The increased power available from the bi-directional pumped OPO described here, coupled with its innocuous effect on living cells, may well prove of great value, not just in the study of plant cells. Photo-damage is the chief limitation of laser scanning microscopy of living cells, and our work suggests a new way of mitigating it.

We conclude from our study that SFM, which can provide wavelengths shorter than those of the Ti:Sapphire laser source, can increase the fluorescence signal intensity from biological specimens at similar illumination powers. Our approach involves SFM of the output from a synchronously pumped optical parametric oscillator with residual pump radiation to generate fs-pulsed output in the red spectral region. We demonstrated the performance of our ultra-short pulsed system using fluorescently labelled tissue and naturally occurring fluorochromes, and, in a comparison with a conventional Ti:Sapphire laser source, we observed more than a 3-fold increase fluorescence signal intensity using our visible laser source in both the DAPI-labelled mouse kidney and the *Hosta* sp leaf epidermis. This alternative to the Ti:Sapphire laser for short-wavelength excitation offers the possibility of reducing the power at the specimen, which may lead to an important reduction in photo-damage of biological tissue.

Our approach to two-photon imaging also has great potential as a replacement for other UV techniques. This includes UV fluorescence lifetime imaging (FLIM)[28, 29] which may increase the viability of the specimen. Also, monitoring of enzyme activity based upon fluorescence anisotropy measurements via spectrally and polarization-resolved imaging, as presented by Bigelow[30] may benefit. Here, two-photon excited anisotropy would provide the added advantage of an enhanced dynamic range, yielding additional information from the images recorded. Both of these proposed applications highlight the widespread impact which is possible from our excitation source.

Finally, we note that imaging based upon two colour two-photon excitation within a specimen (equivalent to SFM) is possible and has been previously demonstrated[31]. However, due to reduced control of the SFM process and dispersion-related issues when using two beams of different wavelengths within a sample, imaging becomes challenging. Also, one of the chosen wavelengths for this process is required to be short (400 nm in the case of Quentmeier), which is a harmful spectral range for biological samples to be exposed to, hence negating one of the fundamental benefits of two photon excitation. Therefore we see SFM prior to the sample as a much more straight-forward and beneficial imaging technique.

ACKNOWLEDGEMENTS

The research leading to these results received funding from the Engineering and Physical Sciences Research Council. The authors would like to thank D. Blatchford, University of Strathclyde, for help with image analysis.

REFERENCES

1. Xu, C., Zipfel, W., Shear, J. B., Williams, R. M. & Webb, W. W. (1996) Multiphoton fluorescence excitation: New spectral windows for biological nonlinear microscopy. *Proc. Natl. Acad. Sci. USA*. **93,** 10763-10768.
2. Träutlein, D., Adler, F., Moutzouris, K., Jeromin, A., Leitenstorfer, A. & Ferrando-May, E. (2008) Highly versatile confocal microscopy system based on a tunable femtosecond Er:fiber source. *J. Biophoton.* **1,** 53–61.
3. Gu, M. (1996) Resolution in three-photon fluorescence microscopy. *Opt. Lett.* **21** 988-990.
4. Barad, Y., Eizenberg, H., Horowitz, M. & Silberberg, Y. (1997) Nonlinear scanning laser microscopy by third harmonic generation. *Appl. Phys. Lett.* **70,** 922–924.
5. Mueller, M., Squier, J. A., Wilson, K. R., & Brakenhoff, G.J. (1998) 3D microscopy of transparent objects using third-harmonic generation. *J. Microsc.* **191,** 266–274.
6. Squier, J. A., Mueller, M., Brakenhoff, G. J., & Wilson, K.R. (1998) Third harmonic generation microscopy. *Opt. Express* **3,** 315–324.
7. Millard, A. C., Wiseman, P. W., Fittinghoff, D. N., Wilson, K. R. & Squier, J. A. (1999) Third-harmonic generation microscopy by use of a compact, femtosecond fiber laser source. *Appl. Opt.* **38,** 7393-7397.
8. Canioni, L., Rivet, S., Sarger, L., Barille, R., Vacher, P. & Voisin, P. (2001) Imaging of Ca2+ intracellular dynamics with a third-harmonic generation microscope. *Opt. Lett.* **26,** 515–517.
9. Debarre, D. et al. (2006) Imaging lipid bodies in cells and tissues using third-harmonic generation microscopy. *Nature Meth*. **3,** 47–53.
10. Sun, C. K., Chu, S. W., Chen, S. Y., Tsai, T. H., Liu, T. M., Lin, C. Y. & Tsai, H. J. (2004) Higher harmonic generation microscopy for developmental biology. *J. Struct. Biol.* **147,** 19–30.
11. Matsuda, H., Fujimoto, Y., Ito, S., Nagasawa, Y., Miyasaka, H., Asahi, T. & Masuhara, H. (2006) Development of near-infrared 35 fs laser microscope and its application to the detection of three- and four-photon fluorescence of organic microcrystals. *J. Phys. Chem. Lett. B* **110,** 1091–1094.
12. Wokosin, D. L., Centonze, V. E., Crittenden, S. & White, J. (1996) Three-photon excitation fluorescence imaging of biological specimens using an all-solid-state laser. *Bioimaging* **4,** 208–214.
13. Keatings, S. R., Zhang, W. & McConnell, G. (2008) Characterization of microscope objective lenses from 1,400 to 1,650 nm to evaluate performance for long-wavelength nonlinear Microscopy Applications. *Microsc. Res. & Tech*. **71,** 517–520.
14. Boyd, R. W. (2008) Nonlinear Optics. *Academic Press*.
15. Tsien, R. Y., Ernst, L. & Waggoner, A. (2006) Fluorophores for confocal microscopy: Photophysics and Photochemistry. *Handbook of Biological Confocal Microscopy* 338-352.
16. Sako, Y., Sekihata, A., Yanagisawa, Y., Yamamoto, M., Shimada, Y., Ozaki, K. & Kusumi, A. (1997) Comparison of two-photon excitation laser scanning microscopy with UV-confocal laser scanning microscopy in three-dimensional calcium imaging using the fluorescence indicator Indo-1. *J. Microscopy* **185**, 9-20.
17. Peng, H., Makarona, E., He., Y., Song, Y.-K., Nurmikko, A. V., Su, J., Ren, Z., Gherasimova, M., Jeon, S.-R., Cui, G. & Han, J. (2004). Ultraviolet LEDs operating in the 340 nm wavelength range and application to time-resolved fluorescence spectroscopy. *Appl. Phys. Lett.* **85**, 1436-1438.
18. McGuinness C D, Sagoo K., McLoskey D. & Birch D. J. S. (2004), A new sub-nanosecond LED at 280 nm: application to protein fluorescence, *Meas. Sci. Technol.* **15**, L19–L22.

19. Xu, C. & Webb, W. W. (1996) Measurement of two-photon excitation cross sections of molecular fluorophores with data from 690 to 1050 nm, *J. Opt. Soc. Am. B* **13**, 481-491.
20. Albota, M. A., Xu, C. & Webb, W. W. (1998) Two-photon fluorescence excitation cross-section of biomolecular probes from 690 to 960 nm. *App. Opt.* **37**, 7352-7356.
21. Norris, G. & McConnell, G. (2010) Relaxed damage threshold intensity conditions and nonlinear increase in the conversion efficiency of an optical parametric oscillator using a bi-directional pump geometry. *Opt. Express.* **18,** 3993-3999.
22. Nguyen, Q. T., Tsai P. S. & Kleinfeld, D. (2006) MPScope: A versatile software suite for multiphoton microscopy. *J. Neuroscience Meth.* **156,** 351-359.
23. Krause, G. H. & Weis, E. (1991) Chlorophyll fluorescence and photosynthesis: the basics. Annu. Rev. Plant Physiol: *Plant Mol. Biol.* **42,** 313-349.
24. Thorne, S. W., Newcomb, E. H., & Osmond, C. B. (1977) Identification of chlorophyll b in extracts of prokaryotic algae by fluorescence spectroscopy. *Proc. Nati. Acad. Sci. USA* **74**, 575-578.
25. Allen, N. S. & Allen, R. D. (1978) Cytoplasmic streaming in green plants. *Ann. Rev. Biophys. Bioeng.* **7,** 497-526.
26. Shimmen, T. & Yokota, E. (2004) Cytoplasmic streaming in plants. *Current Op. in Cell Biol.* **16,** 68–72.
27. Leupold, D., Teuchner, K., Ehlert, J., Irrgang, K-D., Renger, G. & Lokstein, H. (2002). Two-photon excited fluorescence from higher electronic states of chlorophylls in photosynthetic antenna complexes: a new approach to detect strong excitonic chlorophyll a/b coupling. *Biophys. J.* **82**, 1580-1585.
28. Li, Q., Ruckstuhl, T., & Seeger, S. (2004). Deep-UV Laser-Based Fluorescence Lifetime Imaging Microscopy of Single Molecules, *J. Phys. Chem. B,* **108**, 8324-8329.
29. Schneckenburger, H., Wagner, M., Weber, P., Strauss, W. S. L. & Sailer, R. (2004) Autofluorescence Lifetime Imaging of Cultivated Cells Using a UV Picosecond Laser Diode. *J Fluores*. **14,** 649-654.
30. Bigelow, C. E., Vishwasrao, H. D., Frelinger, J. G. & Foster, T. H., (2004) Imaging enzyme activity with polarization-sensitive confocal fluorescence microscopy, *J. Microscopy* **215**(1), 24–33.
31. Quentmeier, S., Denicke, S., & Gericke, K.-H. (2009) Two-Color Two-Photon Fluorescence Laser Scanning Microscopy. *J. Fluoresc.* **19**, 1037-1043.